

## Validation of the Thermal Neutron Scattering Cross Sections for Heavy Water Generated by the Molecular Dynamics Simulation

Haelee Hyun\*, Do Heon Kim and Young-Ouk Lee

Korea Atomic Energy Research Institute, 111, Daedeok-daero 989beon-gil, Yuseong-gu, Daejeon, Republic of Korea

\*Corresponding author: hyunhl@kaeri.re.kr

### 1. Introduction

Although light and heavy water are commonly used as a moderator in nuclear reactors, the existing thermal scattering libraries of light and heavy water have been described by only two different water models (GA model and IKE model). Recently, however, the new model for water has been developed at the Neutron Physics Department at Centro Atómico Bariloche (CAB model) [1], which is applied in the thermal scattering libraries of ENDF/B-VIII.0 for light and heavy water with NJOY2012 code [2]. The significant difference between the CAB model and the existing models is that the CAB model is produced based on the molecular dynamics (MD) simulation to more accurately describe the motions of water molecules. Especially, in case of the CAB model for heavy water, the Sköld correction factor and frequency spectrum of deuterium and oxygen bound in heavy water are calculated by the MD simulation using GROMACS code to consider the coherency and vibration of the molecules of heavy water [3].

In this paper, we also generated the Sköld correction factor and frequency spectrum of deuterium and oxygen to generate the thermal scattering library for heavy water using GROMACS and EPSR code [4] and compared the results by performing ICSBEP [5] benchmark simulation using MCNPX 2.7.0 code [6].

### 2. Calculation method

#### 2.1 Thermal Scattering Law

At thermal energy range, the double differential inelastic scattering cross section for solid, liquid and gas moderator material can be described as a function of the thermal scattering law  $S(\alpha, \beta)$ :

$$\frac{\partial^2 \sigma}{\partial \Omega \partial E} = \frac{\sigma_b}{4\pi kT} \sqrt{\frac{E'}{E}} S(\alpha, \beta), \quad (1)$$

where  $E$  and  $E'$  are the incident and secondary neutron energies,  $\sigma_b$  is the characteristic bound cross section,  $k$  is the Boltzmann constant and  $T$  is the temperature of the material. Also, the thermal scattering law depends on parameters of  $\alpha$  and  $\beta$ . Here  $\alpha$  is the momentum transfer parameter defined as

$$\alpha = \frac{E' + E - 2\sqrt{EE'} \cos \theta}{AKT}, \quad (2)$$

and  $\beta$  is the energy transfer parameter defined as

$$\beta = \frac{E' - E}{kT}, \quad (3)$$

where  $A$  is the mass ratio of the scattering nuclide to the neutron and  $\cos \theta$  is the scattering angle in the laboratory system.

#### 2.2 Sköld correction factor

In order to generate the scattering cross section with the coherent component of deuterium and oxygen, the thermal scattering cross section for heavy water used the Sköld approximation [7,8]. To apply the Sköld approximation, the CAB model has introduced the Sköld correction factors calculated by MD simulation using GROMACS code. In addition, we also calculated the Sköld correction factors using not only GROMACS but also EPSR code. As a result, Fig.1 shows Sköld correction factors. When comparing the Sköld correction factor from GROMACS and EPSR codes with ENDF/B-VIII.0 data, both Sköld correction factors of deuterium show a high consistency. In case of oxygen, however, the Sköld correction factors from GROMACS and EPSR code show lower peaks than ENDF/B-VIII.0 data.

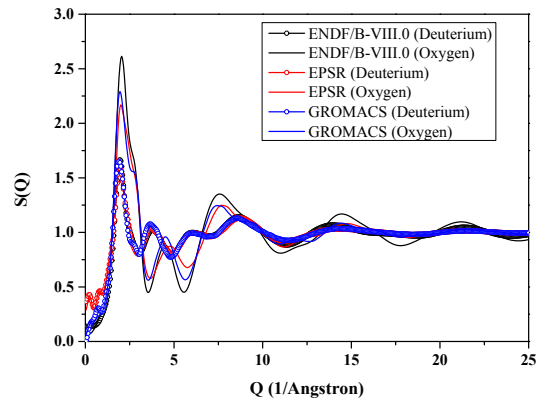


Fig.1. Comparison of Sköld correction factors obtained from ENDF/B-VIII.0 data and calculated by EPSR and GROMACS code (293.6K).

#### 2.3 Frequency Spectrum

The frequency spectrum is obtained from the Fourier transform of the velocity autocorrelation function (VACF). The VACF is calculated using the information of velocities stored in the trajectory file from the result

of GROMACS simulation, which is computed by velacc command in Eq. (4).

$$VACF_{\alpha} = \langle v_{\alpha}(t) \cdot v_{\alpha}(t + \tau) \rangle \quad (4)$$

where  $\tau$  is the time step interval (0.3fs in this paper),  $\langle \cdot \rangle$  is ensemble average of system.

From the VACF, the frequency spectrum can be computed by the Fourier transform with Eq. (5).

$$\rho(\varepsilon) = \frac{M}{3\pi kT} \frac{1}{2\pi} \int_{-\infty}^{\infty} VACF(\tau) \cos(\omega\tau) d\tau \quad (5)$$

where  $\varepsilon = E - E' = \hbar\omega$ ,  $M$  is the mass of each atom.

For heavy water, the frequency distribution is divided into three parts:

1) Diffusion part: it is represented as a diffusion spectrum with the Egelstaff-Schofield model, which could be represented by Eq. (6) [2,9].

$$\rho_{diff}(\omega) = \frac{4cw_t\hbar}{\pi kT} \sqrt{c^2 + 1/4} \cdot \sinh\left(\frac{\hbar\omega}{2kT}\right) \cdot K_1\left\{\frac{\hbar\omega}{kT} \sqrt{c^2 + 1/4}\right\} \quad (6)$$

In Eq. (6),  $K_1(x)$  is a modified Bessel function of the second kind. And  $w_t$  is the translational weight and  $c$  is the diffusion constant, which is provided as an input in LEAPR module of NJOY code.

2) Intermolecular vibration: it is caused by bending and stretching motions between molecules, which is represented as a continuous spectrum. And it can be calculated by subtracting the diffusion spectrum from the generated frequency spectrum.

$$\rho_{cont}(\omega) = \rho(\omega) - \rho_{diff}(\omega) \quad (7)$$

3) Intramolecular vibration: it is caused by bending and stretching motions between atoms inside of the molecule, which is represented as a discrete oscillator. The used values of discrete oscillator of heavy water are listed in Table I.

Table I: Discrete oscillator energies and weights of heavy water (293.6K)

	D in D <sub>2</sub> O	O in D <sub>2</sub> O
First oscillator energy (eV)	0.150	0.150
First oscillator weight	0.14627	0.038288
Second oscillator energy (eV)	0.305	0.305
Second oscillator weight	0.29254	0.076576

The continuous spectrum and the discrete oscillator should be provided as an input of LEAPR module of NJOY code. Figure 2 shows the difference of the continuous spectrums of oxygen and deuterium in heavy water. The solid line represents the continuous spectrum used in the thermal scattering cross section of ENDF/B-VIII.0 and dotted line is the spectrum

calculated by GROMACS. As shown in Fig.2, although both spectrums are based on GROMACS code, they show some differences. The differences might be because the applied simulation conditions (e.g., simulation time, applied ensemble, conditions of equilibration and so on) are different. In addition, the CAB model used the frequency spectrums which combined with the experimental data. In other words, it is not purely from MD simulation. Nevertheless, the frequency spectrums in this work show analogous shape with the frequency spectrum used in the thermal scattering library of ENDF/B-VIII.0. Especially, the peaks of the both spectrums show substantial accordance. The peaks at around 0.6meV and 2~3meV stand for motions of intermolecular bending and stretching of oxygen and deuterium, respectively. In contrast with oxygen, deuterium has third peak at around 4~6meV, which indicates the motion of the librations.

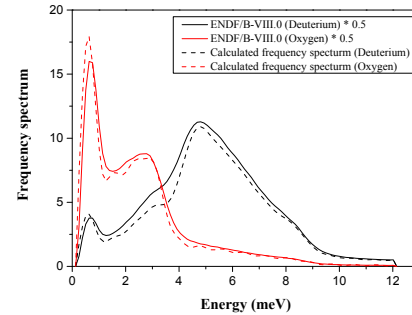


Fig.2. Comparison of continuous spectrums for oxygen and deuterium between the data used in ENDF/B-VIII.0 and calculated by GROMACS code (293.6K).

### 3. Calculation Results

#### 3.1 Comparison of thermal scattering cross sections

Finally, we generated the thermal scattering cross sections for heavy water using NJOY2016 code with new Sköld correction factors and frequency spectrum calculated by MD simulations. As shown in Fig.3, three kinds of thermal scattering cross sections are compared with ENDF/B-VIII.0 data which is used as a reference. The red lined scattering cross sections (FS+ENDF/B-VIII.0) are generated by using the same Sköld correction factor with reference and newly calculated frequency spectrum (FS) in this work. The green lined scattering cross sections (FS+EPSR) are generated by using newly calculated Sköld correction factor by EPSR code and the calculated frequency spectrum. Lastly, the blue lined scattering cross sections (FS+GROMACS) are generated by using newly calculated Sköld correction factor by GROMACS code and calculated frequency spectrum.

As a result, when comparing the reference and FS+ENDF/B-VIII.0, both scattering cross sections agree well above 1meV range. At the lower energy

range than 1meV, the FS+ENDF/B-VIII.0 scattering cross sections of oxygen and deuterium has slightly higher value than the reference. However, the differences are not outstanding. In case of the scattering cross sections of the FS+EPSR and FS+GROMACS, the differences from the reference are more remarkable, which means the scattering cross sections are more significantly affected by the Sköld correction factors. Also, Figure 3 shows the tendency that the scattering cross sections of deuterium which are generated using the Sköld correction factors by GROMACS and EPSR have larger values than the reference under 3meV. However, in case of the scattering cross section for oxygen, the lower values than the reference are observed from 2meV to 9meV. And all scattering cross sections have a common feature that two dips are observed around 3meV and from 10 to 30meV. The first dip comes from the coherence of each atom and the second dip is caused by the effect of O-O interference in D<sub>2</sub>O molecules. Especially, in contrast with the second dip, each scattering cross section shows considerable differences on the first dip range. However, because the neutron flux in thermal systems is much higher at the energy range of the second dip, the description of the second dip is more important.

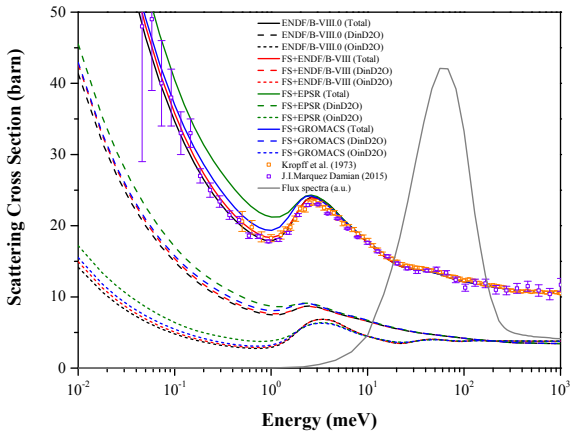


Fig.3. Scattering cross sections for heavy water and the flux spectrum in the thermal system (293.6K).

### 3.2 Criticality Benchmark problems

For estimating the effects of the thermal scattering libraries, 59 heavy water moderated/reflected experiments are taken from the International Handbook of Evaluated Criticality Safety Benchmark Problems (ICSBEP). All of benchmark calculations were done by using Monte Carlo Transport code MCNPX 2.7.0. The ENDF/B-VII.1-based KNE71 library [10] was used for all nuclides except thermal scattering cross sections of D in D<sub>2</sub>O and/or O in D<sub>2</sub>O. All the MCNP benchmark simulations have been carried out at 293.6K. Also, the MCNP runs were terminated after a statistical uncertainty was reduced to below 20 pcm.

Figure 4 shows the differences of calculated  $k_{eff}$  from benchmark  $k_{eff}$  with the thermal scattering libraries of ENDF/B-VIII.0 and generated thermal scattering libraries in categories of the LEU and HEU. The performances of the generated thermal scattering cross sections are similar with the thermal scattering cross section of ENDF/B-VIII.0. As mentioned in section 3.1, because the thermal neutron flux spectrum is biased to the energy range of the second dip, the benchmark results were comparable although the generated scattering cross sections have shown relatively large differences around low energy range.

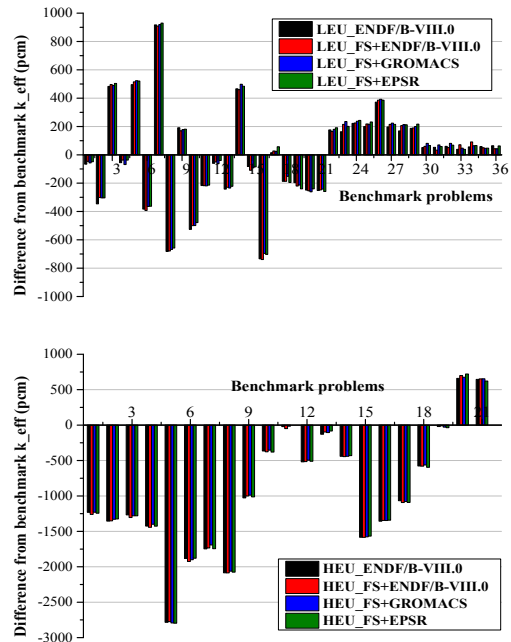


Fig.4. Differences of calculated  $k_{eff}$  from benchmark  $k_{eff}$  with the thermal scattering libraries in categories of the low enriched uranium (LEU) and highly enriched uranium (HEU).

Also, the result of root mean square (RMS) errors for heavy water problems is described in Table II. The total RMS errors of ENDF/B-VIII.0 and generated libraries indicate 0.801~0.808%, which also shows the generated libraries have similar performances with ENDF/B-VIII.0 library in aggregate.

Table II: Comparison of RMS errors relative to benchmark  $k_{eff}$  values among different libraries (Unit: %)

Category (# of cases)	ENDF/B-VIII.0	FS+ENDF/B-VIII.0	FS+GROMACS	FS+EPSR
HEU (21)	1.273	1.279	1.265	1.273
LEU (1)	0.139	0.167	0.172	0.178
LEU (36)	0.327	0.328	0.328	0.328
U233 (1)	0.570	0.549	0.558	0.528
TOTAL (39)	0.805	0.808	0.801	0.805

#### **4. Conclusions**

In this work, we generated the thermal scattering libraries for heavy water by MD simulation. To take into account the coherency of heavy water, we calculated the Sköld correction factors of deuterium and oxygen using GROMACS and EPSR code. In sequence, the frequency spectrum of each atom is also calculated by using GROMACS code to consider the intermolecular and intramolecular vibrations of heavy water. As a result, although the generated thermal scattering cross sections show some discrepancies in comparison with ENDF/B-VIII.0 data below the energy range of 3meV, it is confirmed that the generated libraries show the similar performance with ENDF/B-VIII.0 library after comparing the results of the criticality benchmark simulation.

#### **REFERENCES**

- [1] J. I. Marquez Damian, J. R. Granada, D. C. Malaspina, CAB models for water: a new evaluation of the thermal neutron scattering laws for light and heavy water in ENDF-6 format, *Ann. Nucl. Energy*, 65, 280, 2014.
- [2] A. C. Kahler et al., The NJOY Nuclear Data Processing System, Version 2016, Los Alamos National Laboratory, LA-UR-17-20093, 2016.
- [3] D. Van Der Spoel, E. Lindahl, B. Hess, G. Groenhof, A. E. Mark, H. J. C. Berendsen, GROMACS: Fast, Flexible, and free, *Journal of Computational Chemistry*, 26(16), 1701-1718, 2005.
- [4] A. K. Soper, EPSRshell User Manual, 2009.
- [5] OECD Nuclear Energy Agency, International handbook of evaluated criticality safety benchmark experiments, OECD Nuclear Energy Agency NEA/NSC/DOC(95)03, 2009.
- [6] D. B. Pelowitz, ed. MCNPX USER'S MANUAL, Version 2.7.0, Los Alamos National Laboratory, LA-CP-11-00438, 2011.
- [7] H. L. Hyun, D. H. Kim, Y. O. Lee, Generation and Validation of Thermal Neutron Scattering Cross Sections for Heavy Water by Using New Sköld Correction Factors, *Transactions of the Korean Nuclear Society Autumn Meeting*, 2017
- [8] K. Sköld, Small energy transfer scattering of cold neutrons from liquid argon, *Phys. Rev. Lett.*, 19 (18), 1023-1025, 1967.
- [9] P.A. Egelstaff, P. Schofield, On the Evaluation of the Thermal Neutron Scattering Law, *Nucl.Sci. Eng.*, 12, 260-270, 1962
- [10] D. H. Kim, C. S. Gil, Y. O. Lee, Current Status of ACE Format Libraries for MCNP at Nuclear Data Center of KAERI, *Journal of Radiation Protection and Research*, 41(3), 191-195, 2016